



**HAL**  
open science

## High catalytic activity of Rh nanoparticles generated from cobaltocene and RhCl<sub>3</sub> in aqueous solution

Wenjuan Wang, Roberto Ciganda, Changlong Wang, Ane Escobar, Angel M. Martinez-Villacorta, Maria de Los Angeles Ramirez, Ricardo Hernandez, Sergio E. Moya, Jaime Ruiz, Jean-René Hamon, et al.

► **To cite this version:**

Wenjuan Wang, Roberto Ciganda, Changlong Wang, Ane Escobar, Angel M. Martinez-Villacorta, et al.. High catalytic activity of Rh nanoparticles generated from cobaltocene and RhCl<sub>3</sub> in aqueous solution. *Inorganic Chemistry Frontiers*, 2019, 6 (10), pp.2704-2708. 10.1039/c9qi00742c . hal-02359978

**HAL Id: hal-02359978**

**<https://univ-rennes.hal.science/hal-02359978v1>**

Submitted on 2 Dec 2019

**HAL** is a multi-disciplinary open access archive for the deposit and dissemination of scientific research documents, whether they are published or not. The documents may come from teaching and research institutions in France or abroad, or from public or private research centers.

L'archive ouverte pluridisciplinaire **HAL**, est destinée au dépôt et à la diffusion de documents scientifiques de niveau recherche, publiés ou non, émanant des établissements d'enseignement et de recherche français ou étrangers, des laboratoires publics ou privés.

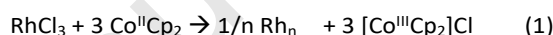
## Highly catalytically active Rh nanoparticles generated from cobaltocene and RhCl<sub>3</sub> in aqueous solution

Wenjuan Wang,<sup>a</sup> Roberto Ciganda,<sup>\*a,b</sup> Changlong Wang,<sup>a</sup> Ane Escobar,<sup>c</sup> Angel M. Martinez-Villacorta,<sup>c</sup> Maria de los Angeles Ramirez,<sup>c</sup> Ricardo Hernández,<sup>b</sup> Sergio Moya,<sup>c</sup> Jaime Ruiz,<sup>a</sup> Jean-René Hamon,<sup>d</sup> and Didier Astruc<sup>\*a</sup>

Rh compounds including Rh nanoparticle are among the most active catalysts for many reactions. Catalytically very reactive small Rh nanoparticles have been generated upon reduction of aqueous RhCl<sub>3</sub> by cobaltocene, characterized, and shown to be very efficient for the test nitrophenol reduction (compared to other metal NPs), generation of hydrogen from ammonia borane hydrolysis, transfer hydrogenation, and benzene hydrogenation. This useful concept of cobaltocenium chloride-stabilized NP catalyst could potentially be efficiently applicable to a variety of other aqueous catalytic systems.

### Introduction

Transition-metal nanoparticles (TMNPs) have attracted much attention from homogeneous to heterogeneous catalysis,<sup>1-9</sup> and among them rhodium nanoparticles (RhNPs) have appeared especially reactive for key reactions for which Earth-abundant metals are not efficient or not sufficiently active catalysts.<sup>10-20</sup> Most RhNPs have so far been synthesized by NaBH<sub>4</sub> reduction of RhCl<sub>3</sub>(H<sub>2</sub>O)<sub>n</sub> that also generates sodium borohydroxyhydride influencing catalysis in an undefined fashion. Here we report the synthesis of RhNPs generated by reduction of RhCl<sub>3</sub> in water using the commercial reducing agent cobaltocene<sup>21</sup> in THF in stoichiometric amount. Cobaltocene is a strong reducing agent<sup>22,23</sup> that has recently been used for the reduction of graphene oxide,<sup>24</sup> the generation of H<sub>2</sub><sup>25</sup> and the reduction of Au,<sup>26</sup> Pd,<sup>26</sup> Cu<sup>27</sup> and Ag<sup>27</sup> salts to metal NPs. It is an electron-reservoir complex,<sup>28,29</sup> i.e. its redox potential  $E^\circ$  (Cp<sub>2</sub>Co<sup>+0</sup>) is very negative (-1.4 V vs. SCE or 0.93 V vs. NHE)<sup>22,23</sup> and both its oxidized and reduced forms are thermally robust.<sup>24</sup> The reduction of RhCl<sub>3</sub> by CoCp<sub>2</sub> was conducted stoichiometrically and follows equation 1, the cobaltocene stoichiometry matching the number of chlorides in the rhodium salt and the decrease of oxidation state from III to 0 leading to the formation of Rh<sup>0</sup>NPs.



### Results and discussion

Cobaltocenium chloride, [Co<sup>III</sup>Cp<sub>2</sub>]Cl,<sup>30</sup> generated in this reaction, is characterized by its absorption at 394 nm in the UV-vis. spectrum (Fig. 1), and it serves as a protecting group surrounding the RhNPs. XPS shows the zero oxidation state of the Rh<sup>0</sup>NPs (Fig. 2). Moreover

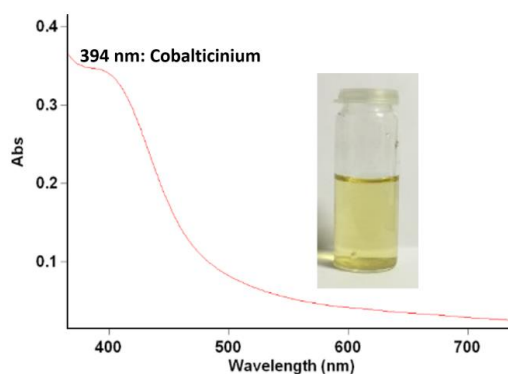


Fig. 1 UV-vis. spectrum of cobaltocenium chloride-stabilized RhNPs.

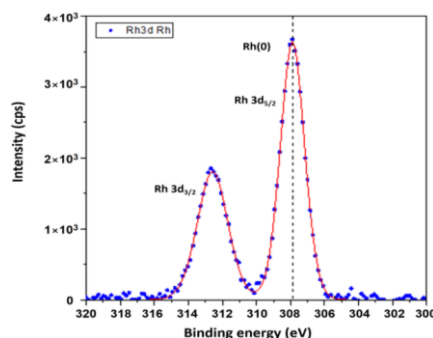


Fig. 2 XPS of cobaltocenium chloride-stabilized RhNPs.

<sup>a</sup> ISM, UMR CNRS 5255, Université de Bordeaux, Talence 33405 Cedex, France. E-mail: didier.astruc@u-bordeaux.fr

<sup>b</sup> Facultad de Química, Universidad del País Vasco, Apdo 1072, 20080 San Sebastián, Spain.

<sup>c</sup> Soft Matter Nanotechnology Lab, CIC biomaGUNE, Paseo Miramón 182, 20014 Donostia-San Sebastián, Gipuzkoa, Spain.

<sup>d</sup> Institut des Sciences Chimiques, UMR CNRS 6226, Université de Rennes 1, 35042 Rennes Cedex, France.

<sup>e</sup> \* Corresponding Author.

<sup>f</sup> Electronic Supplementary Information (ESI) available: UV-vis., XPS, <sup>1</sup>H NMR, TEM images and histograms, recycling catalytic reaction procedures. See DOI: 10.1039/x0xx00000x

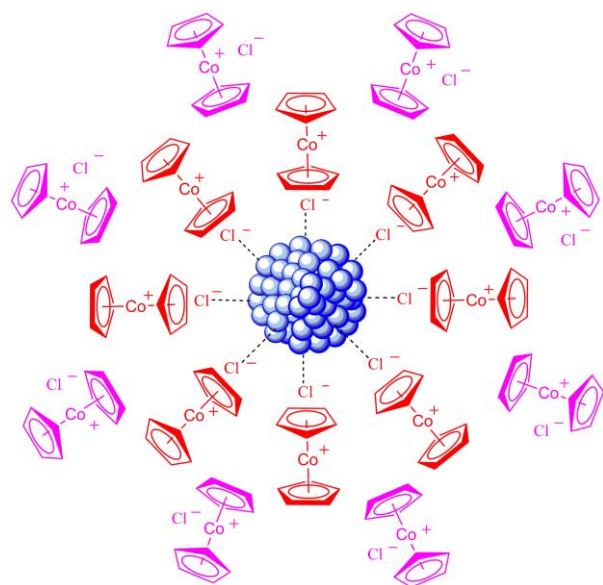


**Fig. 3** Schematic representation of the stabilization of RhNPs by cobalticinium chloride.

Transmission Electron Microscopy (TEM) shows the very small size of  $1.3 \pm 0.1$  nm (Fig. S1), which lets expecting excellent catalytic properties. Previous syntheses of AgNPs by reduction of  $\text{Ag}^{\text{I}}$  salts using cobaltocene have shown that the color of the solution depended on the nature of the counter anion of the precursor  $\text{Ag}^{\text{I}}$  salt. This indicated that the plasmon band of the AgNPs was sensitive to the counter anion coordinated to the AgNP surface.<sup>27</sup> Thus the anions  $\text{Cl}^-$  are weak L (2-electron) ligands for such  $\text{M}^{\text{0}}$ NP surfaces (Fig. 3).

After standing one week at ambient temperature under  $\text{N}_2$ , the cobalticinium stabilized polyanionic RhNPs surrounded by chloride ligands assembled into nanocrystals of 40 to 50 nm size (Fig. 4). It is likely that the formation of these RhNP nanocrystals results from supramolecular electrostatic assembly involving interaction between the polyanionic RhNPs via the cobalticinium linkers. The RhNPs are compared to other MNPs<sup>26,27</sup> using their catalytic efficiency in the reduction by  $\text{NaBH}_4$  of the pollutant 4-nitrophenol (4-NP) to the dye 4-aminophenol (4-AP). See SI.

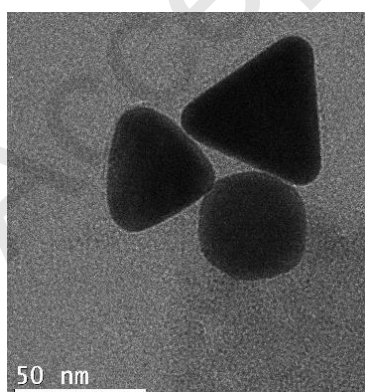


**Fig. 4** Nanocrystals formed by assemblies of cobalticinium chloride-stabilized RhNPs after one week under ambient temperature under  $\text{N}_2$ .

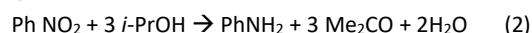
This “green” reaction characterizes the efficiency of the TMNP surface insofar as it was shown by Ballauff’s group that this process involves transformation of the substrates at the TMNP surface as the rate-limiting step.<sup>31,32</sup> Interestingly, the reaction rates (Fig. S8) with 0.2% RhNPs catalyst was found to be remarkably fast with  $k_{\text{app}} = 0.016 \text{ s}^{-1}$ , highlighting a great potential of these nanomaterial as catalysts. The reaction was quantitative at  $35^\circ\text{C}$  in 24 h using only 20 ppm Rh; it was almost as fast as reported with PdNPs, and faster than with AuNPs and other transition metal NPs.<sup>26,27</sup> The RhNP was also tested as catalysts in three other key reactions, transfer hydrogenation of nitrobenzene, hydrolysis of ammonia borane and benzene hydrogenation to cyclohexane, and the results of the homogeneous (semi-heterogeneous) reactions are summarized in Table 1.

**Table 1.** Reactions catalyzed by RhNPs.

	% Rh	T ( $^\circ\text{C}$ )	T (min)	Yield (%)	TON	TOF ( $\text{h}^{-1}$ )
TH $\text{PhNO}_2$	2	80	1440	95 <sup>a</sup>	47.5	2.0
AB hydrolysis	0.05	25	8.5	100	2000	14290
HB	1	40	480	99 <sup>b</sup>	99	12.4

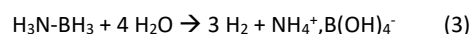
%Rh: mol Rh vs. mol substrate. <sup>a</sup> TH: Transfer hydrogenation of nitrobenzene. AB:  $\text{H}_3\text{N-BH}_3$ . Hydrogenation of Benzene (HB) to cyclohexane was also conducted with graphene oxide support. <sup>a</sup> Isolated yield. <sup>b</sup>  $^1\text{H}$  NMR conversion.

Transfer hydrogenation (TH) is a useful green reaction that allows hydrogenation of substrates with an alcohol as a hydrogen donor instead of dihydrogen.<sup>33,34</sup> For instance TH of nitrobenzene (Table 1, 1st entry) follows equation (2).



This TH reaction using  $\text{H}_2\text{O}/i$ -propanol as both a substrate and the solvent (equation 2) at  $80^\circ\text{C}$  is catalyzed by the RhNPs with 2 mol % metal providing a yield of 95% (Table S1).

Ammonia borane (AB) hydrolysis is a method of choice to generate hydrogen from a hydrogen-rich inorganic hydride under ambient conditions (equation 3), but it needs a good catalyst in order to reach a sufficiently fast reaction under ambient conditions.

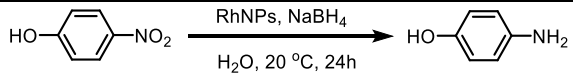


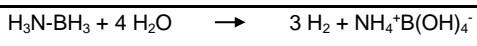
RhNPs are efficient at  $22 \pm 1^\circ\text{C}$  with 0.03 mol% catalyst loading, catalyzing the release of 3 equivalents  $\text{H}_2$  (100 % conversion, Table S2) in 1560 s. In addition, recycling the RhNP catalyst in 0.05 mol% gave 100% yield (Table S2).

The catalyzed hydrogenation (Table 1, HH) of benzene to cyclohexane is an important industrial process<sup>35,36</sup> for which the RhNPs (the most efficient among transition metal NPs, Table S4) catalyzed this reaction at 1 atm  $\text{H}_2$  and  $40^\circ\text{C}$ , providing 100% yield using 0.5 mol% Rh in 16 h or more up to the 3<sup>rd</sup> successive recycling run.

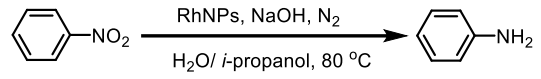
The RhNPs synthesized in this way were also supported on graphene oxide (GO) for these four catalytic reactions and found to be very efficient recyclable catalysts. Table 2 compare the catalytic results of the RhNPs with and without GO support, and Table 3 shows the yields obtained for the TH, AB hydrolysis and benzene hydrogenation upon recycling the RhNP/GO catalyst up to 5 times.

**Table 2.** Compared catalysis results with RhNPs and RhNPs/GO, (AB = hydrolysis of ammonia borane; TH = transfer hydrogenation; HB = hydrogenation of benzene).

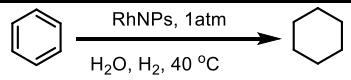
				
4-NP	mol%	T (°C)	t <sub>0</sub> (s)	k <sub>app</sub> (s <sup>-1</sup> )
RhNP	0.2	20	0	0.0158
RhNP/GO	0.02	20	0	0.0163

						
AB	mol%	T (°C)	t (min)	Yield <sup>a</sup> (%)	TON	TOF (h <sup>-1</sup> )
RhNP	0.05	25	8.5	100	2000	14286
RhNP/GO	0.05	25	5.5	100	2000	22222

<sup>a</sup> H<sub>2</sub> release %.

						
TH	mol%	T (°C)	T (min)	Yield <sup>b</sup> (%)	TON	TOF (h <sup>-1</sup> )
RhNP	2	80	1440	95	47.5	2.0
RhNP/GO	1	80	1440	93	93	3.9

<sup>b</sup> Isolated yield.

						
HB	mol%	T (°C)	t (min)	Yield <sup>c</sup> (%)	TON	TOF (h <sup>-1</sup> )
RhNP	1	40	480	99	99	12.4
RhNP/GO	1	40	480	99	99	14.6

<sup>c</sup> <sup>1</sup>H NMR conversion.

**Table 3.** Compared catalysis results with various successive recycling runs with RhNPs/GO.

Catalytic Runs	1 <sup>st</sup>	2 <sup>nd</sup>	3 <sup>rd</sup>	4 <sup>th</sup>	5 <sup>th</sup>
TH (yield <sup>a</sup> , %)	93	91	90	85	80
AB (H <sub>2</sub> release %)	100	100	95	94	90
HB (yield <sup>b</sup> , %)	99	95	92	84	72

(AB = hydrolysis of ammonia-borane; TH = transfer hydrogenation; HB = hydrogenation of benzene). <sup>a</sup> Isolated yield. <sup>b</sup> <sup>1</sup>H NMR conversion.

## Experimental

### General data

All the solvents and chemicals were used as received. The UV-vis. absorption spectra were measured with a Perkin-Elmer Lambda 19 UV-vis. spectrometer. NMR spectra were recorded at 25 °C with a Bruker AC 300 MHz. All the chemical shifts are reported in parts per million ( $\delta$ , ppm) with reference to Me<sub>4</sub>Si for the <sup>1</sup>H NMR spectra. Transmission Electron Microscopy (TEM): The sizes of the TMNPs were determined by TEM using a JEOL JEM 1400 (120 kV) microscope. The TEM samples were prepared by deposition of the nanoparticle suspension (10  $\mu$ L) onto a carbon-coated microscopy copper grid. X-ray Photoelectron Spectroscopy (XPS): System: SPECS SAGE HR; X-Ray source: Al K $\alpha$  non-monochromatic; operated at 12.5 kV and 300 W. Take off angle 90°, at  $\sim 10^{-8}$  Torr. Pass energy for survey spectra 30 eV, 10 eV for narrow scans analysis; spectra are calibrated to CC carbon 285 eV. Analysis is consisted of Shirley background subtraction. Peaks are fitted with symmetrical Gaussian-Lorentzian (GL) line shapes. Samples are prepared by dehydration on the titania coated glass or silica substrates. Titania is selected as a substrate to avoid the overlap of Si and Au. Flash column chromatography was performed using silica gel (300-400 mesh).

### Synthesis of the rhodium nanoparticles (RhNPs)

RhCl<sub>3</sub> (0.84 mg, 4  $\times 10^{-3}$  mmol) was dissolved in 19 mL of Milli-Q water under nitrogen in a standard Schlenk flask and degassed for 10 min, and then [CoCp<sup>2</sup>]<sup>26</sup> (1.5 mg, 8  $\times 10^{-3}$  mmol) in dry THF (1 mL) was quickly injected under nitrogen into the Schlenk flask. The color of the solution changed from colorless to black, indicating the formation of the RhNPs. This synthesis was also scaled up 10-fold.

### RhNPs/rGO Synthesis

The catalyst Rh/rGO was synthesized in water at room temperature. After following the preparation of the cobalticinium-based RhNPs, GO<sup>37,38</sup> was added, and the reaction mixture was stirred for 30 min. The mixture was then aged 3 hours, and the solid was separated, washed and dried at 60 °C overnight. For the recycling study, the catalyst has been recovered by centrifugation, washed, and re-dispersed in water. The reaction then proceeded following the above-mentioned procedure.

### Catalytic reactions

**Reduction of 4-nitrophenol.** 4-NP (1 equiv.) was mixed with NaBH<sub>4</sub> (81 equiv.) in water under air, and the solution containing the RhNP (0.2 mol%) was added. The color of the solution changed from light yellow to dark yellow due to the formation of the 4-nitrophenolate ion. Then, this solution lost its dark yellow color along with the time after addition of the RhNPs. The catalytic 4-NP reduction was monitored via UV-vis. spectroscopy by the decrease of the strong adsorption of the 4-nitrophenolate anion at 400 nm, directly leading to the rate constant.

**Transfer hydrogenation reaction.** A dry Schlenk tube equipped with a magnetic stir bar was charged with nitrobenzene (0.1 mmol) and NaOH (8 mg, 0.2 mmol) under air. Catalytic amounts of a solution of RhNPs were then successively added, and appropriate amount of H<sub>2</sub>O and *i*-propanol were added in order to adjust to a total of 5 mL of solvent (volume ratio of H<sub>2</sub>O/*i*-propanol: 1/4). The mixture was stirred and heated at 80 °C for 24 h. After cooling to r.t., the mixture was extracted three times with ethyl acetate (3  $\times$

20 mL), the organic phase was dried over  $\text{Na}_2\text{SO}_4$ , and the solvent was removed *in vacuo* to obtain the crude products that were analyzed by  $^1\text{H}$  NMR in order to determine the conversions. In parallel, the reaction was checked using TLC. Purification by flash chromatography column was conducted in order to calculate the isolated yields. A reference experiment (Table S1) with only the NaOH base was also conducted following the above-mentioned procedure without adding the RhNP catalyst.  $^1\text{H}$  NMR spectrum (300 MHz,  $\text{CDCl}_3$ ) of aniline.  $\delta_{\text{ppm}}$ : 3.69 (s, 2H), 6.72-6.89 (m, 3H), 7.19-7.26 (m, 2H) (Fig. S3).

**Hydrolysis of ammonia-borane.** A typical dehydrogenation experiment is described here for the hydrolysis of  $\text{H}_3\text{N-BH}_3$  using  $\text{H}_2\text{O}$  as a solvent and 0.03 mol% catalyst loading: A solution of 42.5 mg (1.38 mmol) of  $\text{H}_3\text{N-BH}_3$  in 2.0 ml of  $\text{H}_2\text{O}$  was prepared in a round bottom 40 ml flask fitted with a gas outlet and with a side arm sealed with a tight-fitting septum cap. The flask was connected via the gas outlet to a water-filled gas burette. A solution of RhNPs in 1.0 ml of  $\text{H}_2\text{O}$  was then syringed through the septum, magnetic stirring was connected and timing started. Gas evolution began immediately and the amount of gas evolved was determined periodically by measuring the displacement of water in the burette. 3.0 equivalents of hydrogen occupy 100 mL at atmospheric pressure. Volumes were measured at atmospheric pressure and corrected for water vapor pressure at 20 °C. Table S2 shows the release of hydrogen using different amount of catalyst. The procedure was repeated at different catalyst loadings.

**Hydrogenation of benzene.** All hydrogenation reactions were carried out under mild conditions (40 °C, 1 atm of  $\text{H}_2$ ). A dry tube equipped with a magnetic stir bar was charged with the aqueous solution of RhNPs (5 mL). The tube was closed by a septum, and the system was filled with hydrogen. The substrate, benzene (0.1 mmol), was injected through the septum and the mixture was stirred (1200 rpm). After cooling to r.t., the two phases were separated by decantation, and the organic phase was analyzed by  $^1\text{H}$  NMR in order to determinate the conversion.  $^1\text{H}$  NMR spectrum (300 MHz,  $\text{CDCl}_3$ ) of cyclohexane.  $\delta_{\text{ppm}}$ : 1.49 (s, 12H,  $\text{CH}_2$ ) (Fig. S5).

## Conclusions

In conclusion, RhNPs generated for the first time upon reduction of  $\text{RhCl}_3$  in THF/water by cobaltocene have very small size. This is due to the large reduction driving force between the 19-electron, electron-reservoir complex cobaltocene and  $\text{RhCl}_3$  resulting in its fast reduction. This contrasts with the weak driving force of the 18-electron complex ferrocene<sup>39</sup> that is a poor reductant.<sup>40</sup> RhNPs obtained using cobaltocene are very efficient nanocatalysts for 4-NP reduction to 4-AP without any retention time. RhNPs are also efficient in transfer hydrogenation of nitrobenzene with *i*-propanol,  $\text{H}_2$ -producing ammonia borane hydrolysis, and hydrogenation of benzene. Supporting the cobalticinium chloride-stabilized RhNPs on GO provides a robust and easily recyclable catalyst for these reactions. In sum, the cobalticinium chloride protection provides a fine balance between RhNP protection for stabilization and sufficient open

space around the NPs for catalytic activity. Likewise many other reactions should potentially be efficiently catalyzed by RhNPs or other MNPs prepared using this simple method, and further work along this line with other metals is underway in our laboratories.

## Conflicts of interest

There are no conflicts of interest to declare.

## Acknowledgements

Financial support from the China Scholarship Council of the People's Republic of China (PhD grant to W. W.), (Gobierno Vasco (postdoctoral scholarship to R.C.), the Universidad del País Vasco, the University of Bordeaux and CIC biomaGUNE is gratefully acknowledged.

## Notes and references

- 1 L. M. Bronstein and Z. B. Shifrina, *Chem. Rev.*, 2011, **111**, 5301.
- 2 V. Polshettiwar and R. S. Varma, *Green Chem.*, 2010, **12**, 743.
- 3 V. S. Myers, M. G. Weir, E. V. Carino, D. F. Yancey, S. Pande and R. M. Crooks, *Chem. Sci.*, 2011, **2**, 1632.
- 4 A. Corma, A. Leyva-Perez and M. J. Sabater, *Chem. Rev.*, 2011, **111**, 1657.
- 5 M. Sankar, N. Dimitratos, P. J. Miedziak, P. P. Wells, C. J. Kiely and G. J. Hutchings, *Chem. Soc. Rev.*, 2012, **41**, 8099–8139.
- 6 M. Haruta, *Angew. Chem. Int. Ed.*, 2014, **53**, 52.
- 7 R. Ye, B. Yuan, J. Zhao, W. T. Ralston, C. Y. Wu, E. Unel Barin, F. D. Toste and G. A. Somorjai, *J. Am. Chem. Soc.*, 2016, **138**, 8533.
- 8 D. Astruc, F. Lu and J. Ruiz, *Angew. Chem., Int. Ed.*, 2005, **44**, 7852.
- 9 M. – C. Daniel and D. Astruc, *Chem. Rev.*, 2004, **104**, 293.
- 10 A. R. Tao, S. Habas and P. D. Yang, *Small*, 2008, **4**, 310.
- 11 M. Dhiman, B. Chalke and V. Polshettiwar, *ACS Sustain. Chem. Eng.*, 2015, **3**, 3224.
- 12 X. Zhang, X. Q. Li, M. E. Reish, D. Zhang, N. Q. Su, Y. Gutierrez, F. Moreno, W. T. Yang, H. O. Everitt and J. Liu, *Nano Lett.*, 2018, **18**, 1714.
- 13 A. M. Watson, X. Zhang, R. A. de la Osa, J. M. Sanz, F. Gonzales, F. Moreno, G. Finkelstein, J. Liu and H. O. Everitt, *Nano Lett.*, 2015, **15**, 1095.
- 14 L. B. Wang, H. L. Li, W. B. Zhang, X. Zhao, J. X. Qiu, A. W. Li, X. S. Zheng, Z. P. Hu, R. Si and J. Zeng, *Angew. Chem., Int. Ed.*, 2017, **56**, 4712.
- 15 S. Akbayak, Y. Tonbul and S. Ozkar, *Appl. Catal. B-Environmental.*, 2016, **198**, 162.
- 16 Q. L. Yao, Z. H. Lu, Y. S. Jia, X. S. Chen and X. Liu, *Int. J. Hydrog. Energy*, 2015, **40**, 2207.
- 17 G. Chacon and J. Dupont, *ChemCatChem*, 2019, **11**, 333.
- 18 F. Gao, Y. P. Zhang, P. P. Song, J. Wang, T. X. Song, C. Wang, L. Song, Y. Shiraishi and Y. K. Du, *J. Mater. Chem. A*, 2019, **7**, 7891.
- 19 L. Liu, J. F. Li, Y. J. Ai, Y. H. Liu, J. L. Xiong, H. D. Wang, Y. J. Qiao, W. R. Liu, S. C. Tan, S. F. Feng, K. P. Wang, H. B. Sun and Q. L. Liang, *Green Chem.*, 2019, **21**, 1390.
- 20 H. B. Zou, B. Jin, R. W. Wang, Y. B. Wu, H. Q. Yang and S. L. Qiu, *J. Mater. Chem. A*, 2018, **6**, 24166.
- 21 E. O. Fischer, *Angew. Chem., Int. Ed.*, 1952, **64**, 620-621.
- 22 N. G. Connelly and W. E. Geiger, *Chem. Rev.*, 1996, **16**, 877.

- 23 D. Astruc, *Electron Transfer and Radical Processes in Transition Metal Chemistry*. Wiley, New York, 1995.
- 24 M. M. MacInnes, S. Hlynchuk, S. Acharya, N. Lehnert and S. Maldonado, *ACS Appl. Mater. Interfaces*, 2018, **10**, 2004.
- 25 I. H. Kwak, H. G. Abbas, I. S. Kwon, Y. C. Park, J. Seo, M. K. Cho, J.-P. Ahn, H. W. Seo, J. Park and H. S. Kang, *J. Mater. Chem. A*, 2019, **7**, 8101.
- 26 F. Fu, Q. Wang, R. Ciganda, A. M. Martinez-Villacorta, A. Escobar, S. Moya, E. Fouquet, J. Ruiz and D. Astruc, *Chem. Eur. J.*, 2018, **24**, 6645.
- 27 F. Fu, R. Ciganda, Q. Wang, A. Tabey, C. Wang, A. Escobar, A. M. Martinez-Villacorta, R. Hernandez, S. Moya, E. Fouquet, J. Ruiz and D. Astruc, *ACS Catal.*, 2018, **8**, 8100.
- 28 A. M. Madonik and D. Astruc, *J. Am. Chem. Soc.*, 1984, **196**, 2437.
- 29 M-H. Desbois, D. Astruc, J. Guillin, F. Varret, A. X. Trautwein, and G. Villeneuve, *J. Am. Chem. Soc.*, 1989, **111**, 5800.
- 30 G. Wilkinson, *J. Am. Chem. Soc.*, 1952, **74**, 6148.
- 31 S. Wunder, Y. Lu, M. Albrecht, M. Ballauff, *ACS Catal.*, 2011, **1**, 908.
- 32 Y. Mei, Y. Lu, F. Polzer, M. Ballauff and M. Dreshler, *Chem. Mater.*, 2007, **19**, 1062.
- 33 R. A. Farrar-Tobar, B. Wozniak, A. Savini, S. Hinze, S. Tin, J. G. de Vries, *Angew. Chem. Int. Ed.*, 2019, **58**, 1129.
- 34 N. Castellanos-Blanco, A. Arévalo and J. J. García, *Dalton Trans.*, 2016, **45**, 13604.
- 35 F. Dobert and Gaube, *J. Catal. Lett.*, 1995, **31**, 431.
- 36 P. Kluson and L. Cerveny, *Appl. Catal.* 1995, **128**, 13.
- 37 J. G. Radich and P. V. Kamat, *ACS Nano*, 2013, **7**, 5546.
- 38 C. Wang, R. Ciganda, L. Yate, S. Moya, L. Salmon, J. Ruiz and D. Astruc, *J. Mater. Sci.*, 2017, **52**, 9465.
- 39 D. Astruc, *Eur. J. Inorg. Chem.*, 2017, **1**, 6.
- 40 R. Ciganda, J. Irigoyen, D. Gregurec, R. Hernández, S. Moya, C. Wang, J. Ruiz, D. Astruc, *Inorg. Chem.* 2016, **55**, 6361.